Hassirian *et al. Annals of Microbiology* (2022) 72:6
https://doi.org/10.1186/s13213-022-01665-9

Annals of Microbiology

UNIVERSITÀ DEGLI STUDI DI MILANO

ORIGINAL ARTICLE

Open Access

Nanoliposome-encapsulated phenolic-rich fraction from *Alcea rosea* as a dietary phytobiotic in mice challenged by *Escherichia coli*

Niloofar Hassirian[1†], Ehsan Karimi[1*†] and Ehsan Oskoueian[2†]

Abstract

Purpose: This research was performed to evaluate the antibacterial and health-promoting potentials of nanoliposome-encapsulated phenolic-rich fraction (PRF) from *Alcea rosea* leaves, as a dietary phytobiotic, in mice as challenged by enteropathogenic *Escherichia coli* (*E. coli*; O157: H7).

Method: The PEF was encapsulated in nanoliposomes (PEF-NLs), and the phenolic profiling of PEF-NLs was confirmed by HPLC. Next, 40 white male balb/c mice were assigned to four treatment groups to assess the antibacterial potential of PEF-NLs by measuring the blood parameters and the liver's lipid peroxidation in the mice as a result of the infection caused by *E. coli*. Finally, the expression of cyclooxygenase 2 (COX2), inducible nitric oxide synthase (iNOS), superoxide dismutase (SOD), and glutathione peroxidase (GPx) were determined in the mice's ileum tissues. A real-time PCR was used to analyze the relative fold changes in the population of *E. coli* in the ileum.

Results: The overall results demonstrated that the nanoliposome-loaded PRF contained gallic acid, salicylic acid, pyrogallol, cinnamic acid, catechin, naringin, and ferulic acid. The *E. coli* intervention impaired the mice's weight gain, food intake, liver enzymes, lipid peroxidation, and the ileum's morphometric characteristics. The challenge also upregulated the inflammatory genes (COX2, iNOS), downregulated the antioxidant-related genes (SOD and GPx), and increased the population of *E. coli* in the ileum. The dietary inclusion of the nonencapsulated PRF and the nanoliposome-encapsulated PRF, at the concentration of 10 mg TPC/kg BW/day, improved these parameters. However, compared to nonencapsulated PRF, the nanoliposome-encapsulated PRF appeared to be more effective in improving the health parameters in mice.

Conclusion: As a promising phytobiotic, the nanoliposome-encapsulated PRF could play a critical role against the *E. coli* infection in mice probably due to the increase in the higher intestinal solubility, bioavailability, and absorption of phenolic compounds encapsulated in the nanoliposome carrier.

Keywords: Phytogenic, Phytobiotic, Enteropathogen, Natural antibiotic, Antibiotic replacing agent, Encapsulation

Background

Various antibiotics, such as β-lactams, chloramphenicol, tetracyclines, aminoglycosides, macrolides, glycopeptides, quinolones, streptogramins, oxazolidinones, lipopeptides, and mutilins, have been developed to cure infectious diseases (Fischbach and Walsh 2009). As a

*Correspondence: ehsankarimi@mshdiau.ac.ir
†Niloofar Hassirian, Ehsan Karimi and Ehsan Oskoueian contributed equally to this work.
[1] Department of Biology, Mashhad Branch, Islamic Azad University, Mashhad, Iran
Full list of author information is available at the end of the article

major cause of human death, infectious diseases have become an increasingly important public health issue worldwide. The increase is mainly attributed to the development of antibiotic-resistant strains, including, but not limited to, *Pseudomonas aeruginosa*, *Escherichia coli* (*E. coli*), *Proteus vulgaris*, *Staphylococcus aureus*, *Shigella dysenteriae*, and *Salmonella typhi* (Hwang et al. 2017; Vadhana et al. 2015). Such antibiotic resistance may cause higher drug prices and mortality rates (Friedman et al. 2016; Frieri et al. 2017); hence, it has spearheaded the search for new alternative sources of antimicrobial agents that are effective, yet cheap and accessible, and that possess few to no undesirable side-effects, such as bioactive constitutes of plants (Górniak et al. 2019; Gutiérrez-del-Río et al. 2018; Mostafa et al. 2018).

Several studies have shown that natural products contain higher chemical novelty than chemically-synthesized products; this, in turn, underscores the need to conduct further research on active compounds, such as flavonoid and phenolic compounds, in plants. These compounds have been reported to play a significant role, as antimicrobial agents, in therapeutic applications. They offer major opportunities for finding new lightweight molecules that are active against microbes (Anand et al. 2019; Hadi et al. 2017).

Alcea rosea L. (A. rosea), also known as Hollyhock, belongs to the Malvaceae family. It is an ornamental plant widely grown in the eastern Mediterranean to central Asia (Khoshnamvand et al. 2019). Most of the subspecies have been reported to exist mainly in Iran and Turkey (Azab 2017). Different aerial parts of these plants, including the seed, root, leaves, and flower, have been applied in traditional medicine for irritated stomach, throat pain, fever, and kidney pain. The major natural constitutes isolated from different parts of this medicinal plant including ferulic, vanillic, syringic, isoquercitrin, kaempferol, caffeic, and p-Coumaric acid exhibited a wide range of biological potential (Nicolau and Gostin 2016; Zhang et al. 2015).

These plants contain antimicrobial and anti-inflammatory agents (Abdel-salam et al. 2018; Azab 2017). Most of such biological properties in this plant are associated with natural bioactive compounds, especially phenolic compounds. Phenolic compounds are considered abundant and interesting micronutrients due to such pharmaceutical properties as a natural antioxidant and antimicrobial potential (Acosta-Estrada et al. 2014; Cianciosi et al. 2018). In line with this study, previous researches reported that extract obtained from leaves of *Alcea rosea* L. using different solvents (hexane, ethanol, ethyl acetate, and water) exhibited notable antibacterial activities against several pathogenic bacteria such as *Escherichia coli*, *Staphylococcus aureus*, *Staphylococcus epidermidis*, *Salmonella typhimurium*, *Enterobacter cloacae*, *Enterococcus faecalis*, and *Pseudomonas aeruginosa* (Hashemi et al. 2021; Lim 2014; Tuba et al. 2010). Another study indicated that the root extracts decrease the number of kidney calcium oxalate deposits in ethylene glycol-induced kidney calculi in rats (Ahmadi et al. 2012).

However, the widespread use of phenolic compounds has been limited due to their low solubility resulting in poor absorption and biological activities. Previous studies revealed that different carriers like liposomes could improve solubility and enhance the bioactivity of these natural components (Rafiee et al. 2017). Nanoliposomes consist of phospholipid bilayers that are microscopic carriers that can control the release of natural bioactive compounds like polyphenols to the target place and enhance the effectiveness and cellular uptake of the encapsulated natural constitute (Hasan et al. 2014a). The liposome delivery system has also been shown to improve the effectiveness of the bioactive compound by enhancing the solubility, bioavailability, and preventing unwanted interactions with other molecules. The liposome can also provide a slow release of an encapsulated natural constitute resulting in sustained exposure to the site of action and increase efficacy (Figueroa-Robles et al. 2021). Thus, encapsulation using liposomal technology as carriers is aimed to enhance the bioavailability of pharmaceuticals and nutraceuticals potent polyphenols (Aditya et al. 2017).

Liposomes comprise one or more spherical lipid bilayers that encapsulate bioactive molecules. They can entrap both the lipophilic and the hydrophilic molecules in their unique individual structure (Aditya et al. 2017), where the lipophilic molecules are inserted into the phospholipid bilayer membrane and the hydrophilic molecules are encapsulated into the aqueous center of the liposome. In other words, the nanoliposomes' internal compartment is filled with a polar liquid media, such as a buffer or water containing dissolved hydrophilic compounds (Emami et al. 2016). Nanoliposomes, as targeted-drug delivery systems, are the most applicable nano-carriers in the pharmaceutical industry; they could improve the therapeutics' efficiency in a wide range of biomedical applications. Moreover, nanoliposomes facilitate the cellular uptake of their contents and stabilize them efficiently (Ozkan et al. 2019; Salimi 2018). Hence, the present work aimed to synthesize a nanoliposome-encapsulated phenolic-rich fraction from *A. rosea* and evaluate its antibacterial and health-promoting activities in mice as challenged by enteropathogenic *E. coli* (O157: H7).

Results and discussion

Fractionation and total phenolic determination

The fractionation, using different polarity solvents, resulted in the extraction of a large amount of phenolic compounds from the *A. rosea* leaves in different quantities, with the highest phenolic compounds detected in ethyl acetate fraction 26.1 ± 4.36 followed by n-butanol (16.7 ± 3.29) > water (12.6 ± 3.94) > chloroform (8.3 ± 2.76) > hexane (7.5 ± 2.63) mg GAE/g DW of the extract, respectively. The ethyl acetate fraction was found to contain the highest amount of phenolic compounds; therefore, it was named the phenolic-rich fraction (PRF) and was used for further experiments. Several early studies indicated that the phenolic compounds are moderately polar compounds which is why they tend to accumulate in the fraction of medium polarity such as ethyl acetate. Similar observations were reported by early studies who observed the highest total phenolic content in the ethyl acetate fraction among other solvents used including hexane, chloroform, n-butanol, and water (Abdelwahab et al. 2010; Ju et al. 2012; Kaur et al. 2008; Mariem et al. 2014; Olatunji et al. 2017).

Physicochemical characteristics of PRF-loaded nanoliposome

Table 1 shows the characteristics of the nanoliposomes-loaded PRF. The particle size is an important factor in the stability and bioavailability of nanoliposomes. In this study, the particle size was 254.3 ± 7.91 nm, representing the nanometer size of the particles. As shown in Table 1, the PDI values were reported as 0.31 ± 0.08, indicating a homogenous dispersion (Hasan et al. 2014b). Based on the classification proposed by Kumar and Dixit (2017), the zeta potential values indicated moderate stability in the colloidal dispersion (34.04 ± 0.6 mV). The FESEM image, presented in Fig. 1, displayed the spherical shape of nanoliposomes. Nanoliposomes contained total phenolic compounds of 1.9 ± 0.12 mg GAE/g DW.

Table 1 Physical and phytochemical characteristics of nanoliposome-loaded phenolic-rich fraction from *A. rosea*

Particle size (nm)	Polydispersity index (PDI)	Zeta potential (mV)	Total phenolics (mg GAE/g DW)
254.3 ± 7.91	0.31 ± 0.08	− 34.04 ± 0.6	1.9 ± 0.12

Phenolic compounds analysis

Table 2 demonstrates the profiling of the phenolic compounds within nanoliposomes. The results showed the existence of various types of phenolic compounds in nanoliposomes, with the cinnamic acid and gallic acid as the main and most abundant phenolic compounds with respective values of 805 ± 8.2 and 728.2 ± 3.1 µg/g DW.

Animal trial

The average daily weight gain and food intake are shown in Table 3. The results revealed that the *E. coli* challenge (T2) significantly impaired ($p < 0.05$) the daily weight gain and food intake as compared to the unchallenged group (T1). Moreover, the dietary addition of the phytogenic compounds, in the form of nonencapsulated and nanoliposome-encapsulated PRFs, improved these parameters significantly ($p < 0.05$) in the *E. coli*-challenged mice in groups T3 and T4. The results unveiled that the dietary incorporation of nanoliposome-encapsulated PRF-based phytogenic compounds was more effective than its nonencapsulated PRF counterpart in improving the daily weight gain and food intake. Such improvements could be associated with the antioxidant and antibacterial activity of the bioactive compounds (e.g., gallic acid, salicylic acid, pyrogallol, cinnamic acid, catechin, naringin, and ferulic acid) detected in the PRF.

Liver enzymes and lipid peroxidation analysis

The results from the liver enzymes analysis and lipid peroxidation in the liver tissue are presented in Table 4. As shown, the liver enzymes and lipid peroxidation significantly increased ($p < 0.05$) as a result of the *E. coli* challenge as compared to the unchallenged group. Furthermore, the inclusion of the nonencapsulated PRF and the nanoliposome-encapsulated PRF alleviated the liver enzymes (SGOT, SGPT, ALP) and the lipid peroxidation in the liver tissue to a great extent ($p < 0.05$). In line with the results obtained from daily weight gain and food intake, we observed that supplying PRF in the form of

Table 2 Phenolic compounds presented in the nanoliposome-loaded phenolic-rich fraction from *A. rosea*

Phenolic compounds contents (µg/g DW)						
GA	SA	PY	CA	CT	NA	FE
728.2 ± 3.1	577 ± 6.4	411 ± 6.5	805 ± 8.2	236 ± 5.7	342 ± 3.3	221 ± 6.2

GA gallic acid, *SA* salicylic acid, *PY* pyrogallol, *CA* cinnamic acid, *CT* catechin, *NA* naringin, *FE* ferulic acid. The analyses were performed in triplicates

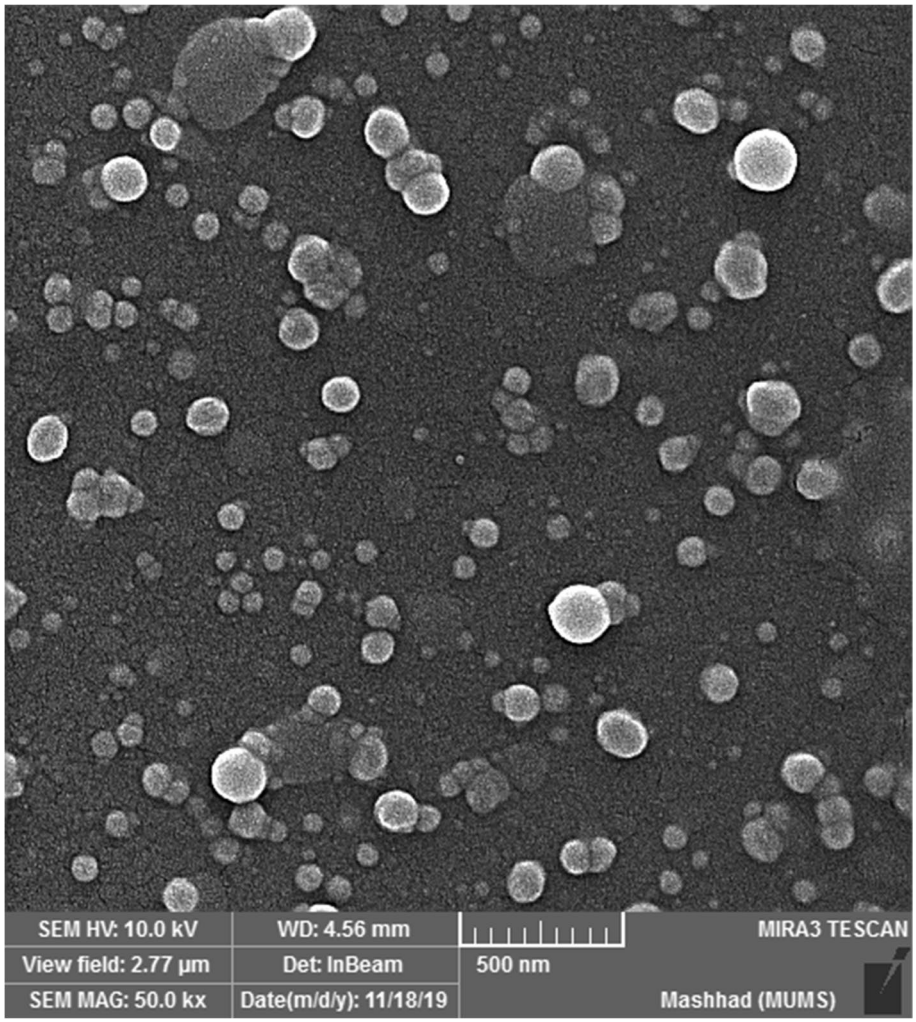

Fig. 1 The FESEM analysis of nanoliposome-loaded phenolic-rich fraction from *A. rosea*

Table 3 The average changes in weight and food intake

Average	T1	T2	T3	T4	SEM
Average daily weight gain (g)	0.23^{a}	0.16^{cd}	0.18^{c}	0.21^{ab}	0.06
Average daily food intake (g)	3.5^{a}	2.6^{c}	2.9^{bc}	3.1^{b}	0.12

T1: normal diet. T2: normal diet + infection by *E. coli* (O157:H7) on day 21. T3: a normal diet enriched by a nonencapsulated phenolic-rich fraction (10 mg TPC/kg BW/day) + infection by *E. coli* (O157:H7) on day 21. T4: a normal diet enriched by a nanoliposome-encapsulated phenolic-rich fraction (10 mg TPC/kg BW/day) + infection by *E. coli* (O157:H7) on day 21

Letters a, b, c, and d in the same row represent a significant difference ($p < 0.05$)

The analyses were performed in triplicates

nanoliposome-encapsulated PRF was more effective in modulating the liver enzymes and lipid peroxidation as compared to the nonencapsulated PRF. The alleviation of liver enzymes and lipid peroxidation by using nanoliposome-encapsulated PRF through dietary regimen could be associated with the antioxidant and antibacterial activity of the gallic acid, salicylic acid, pyrogallol, cinnamic acid, catechin, naringin, and ferulic acid present in the nanoliposomes. These results revealed that the infecting mice with *E. coli* reduced the appetite and induced weight loss due to gastroenteritis. The *E. coli* induced gastroenteritis through adherence to the intestinal mucosa and initiating to produce enterotoxin and cytotoxins (Hassan et al. 2021). The enterotoxin and cytotoxins reduced

Table 4 The results of liver enzymes analysis and lipid peroxidation in the liver tissue

Parameters	T1	T2	T3	T4	SEM
SGOT (IU/L)	129.8^{d}	173.1^{a}	157.2^{b}	142.1^{c}	4.67
SGPT (IU/L)	106.1^{d}	169.4^{a}	136.4^{b}	124.6^{c}	5.63
ALP (IU/L)	147.3^{d}	215.6^{a}	171.4^{b}	158.9^{c}	7.42
MDA* (%)	100^{d}	173^{a}	156^{b}	142^{c}	4.49

T1: normal diet. T2: normal diet + infection by *E. coli* (O157:H7) on day 21. T3: a normal diet enriched by a nonencapsulated phenolic-rich fraction (10 mg TPC/kg BW/day) + infection by *E. coli* (O157:H7) on day 21. T4: a normal diet enriched by a nanoliposome-encapsulated phenolic-rich fraction (10 mg TPC/kg BW/day) + infection by *E. coli* (O157:H7) on day 21

Letters a, b, c, and d in the same row represent a significant difference ($p < 0.05$)

*Expressed as malondialdehyde changes relative to the control group (T1)

The analyses were performed in triplicates

the appetite, increased weight loss, and elevated the liver enzymes and lipid peroxidation which resulted in induction of systemic inflammation and oxidative stress. The nanoliposomes used in this study could improve weight gain and alleviate the liver enzymes production and lipid peroxidation in the mice challenged by *E. coli*. This improvement could be associated with the presence of antimicrobial, antioxidant, anti-inflammatory, and hepatoprotective activity of phenolic compounds present in the nanoliposomes (Sarı et al. 2019). Moreover, the higher biological activity of nanoliposome-encapsulated PRF could be associated with the higher intestinal solubility and absorption of nanoliposome-encapsulated PRF as compared to the nonencapsulated PRF.

Histopathology and morphometric analyses

The histopathological characteristics of the mice's liver, kidney, and ileum, after the treatment by pathogenic bacteria, the nonencapsulated PRF, and the nanoliposome-encapsulated PRF, are presented in Fig. 2. The results showed normal architecture of the liver, kidney, and ileum in the control group (T1). The administration of *E. coli* (O157: H7) on day 21 failed to induce any meaningful histomorphological changes in the tissues of the liver and kidney. Having used the nonencapsulated and the nanoliposome-encapsulated PRFs, we further observed that the *E. coli* (O157: H7) intervention failed to affect the histomorphology of the liver and kidney.

The morphometric analysis of the ileum, including the villus height and width, the crypt depth, and the number of goblet cells in the experimental group, is reported in Table 5. While the villus height and width, and the number of goblet cells declined significantly ($p < 0.05$) in the group challenged by *E. coli*, the crypt depth increased considerably ($p < 0.05$). The dietary inclusion of 10 mg TPC/kg BW/day of the nonencapsulated PRF and the nanoliposome-encapsulated PRF significantly improved ($p < 0.05$) the villus height and width and the crypt depth as well as the quantity of the goblet cells. Similarly, earlier studies reported the role of the plant's bioactive compounds in promoting the morphostructure of the ileum in enteropathogens of the infected or uninfected rabbits (Pogány Simonová et al. 2020), pigs (Nofrarias et al. 2006), rats (Erlwanger and Cooper 2008), and the broiler chickens (Khan et al. 2017).

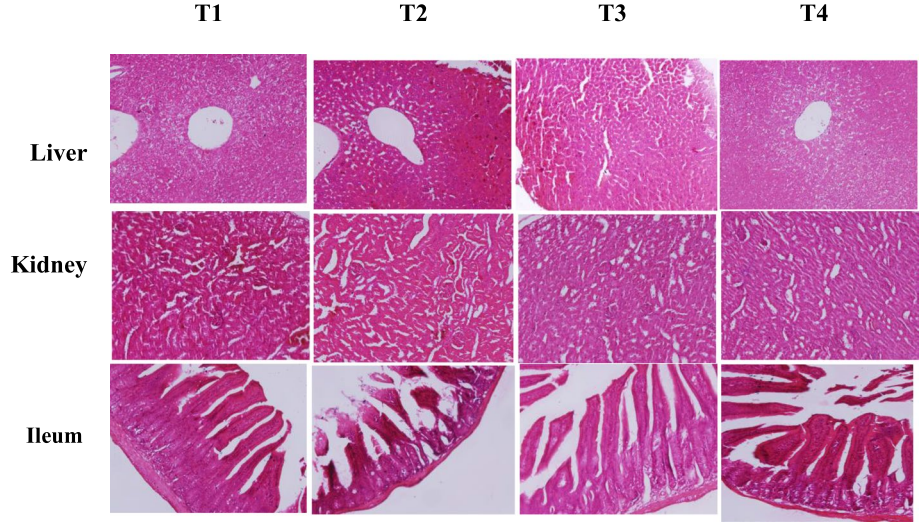

Fig. 2 Histopathological analysis of the liver, kidney, and ileum of the mice under different treatment conditions. T1: normal diet. T2: normal diet + infection by *E. coli* (O157: H7) on day 21. T3: a normal diet enriched by a nonencapsulated phenolic-rich fraction (10 mg TPC/kg BW/day) + infection by *E. coli* (O157: H7) on day 21. T4: a normal diet enriched by a nanoliposome-encapsulated phenolic-rich fraction (10 mg TPC/kg BW/day) + infection by *E. coli* (O157: H7) on day 21

Table 5 Morphometric analysis of the ileum under different treatment conditions

Parameters	T1	T2	T3	T4	SEM
Villus height (μm)	438.2^{a}	327.6^{d}	396.2^{c}	414.8^{b}	6.41
Villus width (μm)	115.1^{a}	89.6^{d}	94.2^{c}	100.7^{b}	4.23
Crypt depth (μm)	140.3^{d}	192.8^{a}	182.1^{b}	169.7^{c}	4.66
Mean number of goblet cells	5.5^{a}	3.7^{c}	4.3^{b}	4.4^{b}	0.47

T1: normal diet. T2: normal diet + infection by *E. coli* (O157: H7) on day 21. T3: a normal diet enriched by a nonencapsulated phenolic-rich fraction (10 mg TPC/kg BW/day) + infection by *E. coli* (O157: H7) on day 21. T4: a normal diet enriched by a nanoliposome-encapsulated phenolic-rich fraction (10 mg TPC/kg BW/day) + infection by *E. coli* (O157:H7) on day 21

Letters a, b, c, and d in the same row represent a significant difference ($p < 0.05$)

The analyses were performed in triplicates

Table 6 The gene expression analysis of mice under different treatments

Genes	Fold changes				SEM
	T1	T2	T3	T4	
COX2	1.0^{d}	$+5.1^{a}$	$+3.1^{b}$	$+1.1^{c}$	0.06
iNOS	1.0^{d}	$+3.1^{a}$	$+2.2^{b}$	$+1.3^{c}$	0.17
SOD	1.0^{c}	-1.3^{d}	$+1.2^{b}$	$+1.9^{a}$	0.09
GPx	1.0^{c}	-1.6^{d}	$+0.4^{b}$	$+1.3^{a}$	0.14

T1: normal diet. T2: normal diet + infection by *E. coli* (O157: H7) on day 21. T3: a normal diet enriched by a nonencapsulated phenolic-rich fraction (10 mg TPC/kg BW/day) + infection by *E. coli* (O157: H7) on day 21. T4: a normal diet enriched by a nanoliposome-encapsulated phenolic-rich fraction (10 mg TPC/kg BW/day) + infection by *E. coli* (O157: H7) on day 21

Letters a, b, c, and d in the same row represent a significant difference ($p < 0.05$)

The analysis was performed in triplicates

Gene expression analysis

The expression of COX2 and iNOS, as major biomarkers of inflammation, and SOD and GPx genes, as biomarkers of the antioxidant activity in the ileum, are shown in Table 6. Compared to the intact group (T1), the infection caused by *E. coli* (T2) significantly ($p < 0.05$) upregulated the expression of COX2 and iNOS and downregulated the expression of SOD and GPx in the experimental group. The dietary addition of 10 mg TPC/kg BW/day of the nonencapsulated PRF and the nanoliposome-encapsulated PRF could greatly suppress ($p < 0.05$) COX2 and iNOS, as inflammatory markers, and enhance the expression of SOD and GPx genes, as an indicator of cellular antioxidant redox potential. The higher intestinal solubility, bioavailability, and absorption of nanoliposome-encapsulated PRF resulted in significant ($p < 0.05$) downregulation in the inflammation and upregulation in antioxidant-related genes as compared to the mice who received non-encapsulated PRF. Apart from that, the regulation of the inflammatory and antioxidant-related genes was associated with the anti-inflammatory and antioxidant activities of the bioactive compounds found in PRF (e.g., gallic acid, salicylic acid, pyrogallol, cinnamic acid, catechin, naringin, ferulic acid) (Rubió et al. 2013).

E. coli population analysis

Figure 3 illustrates the relative changes in the *E. coli* population under different treatments. As compared to the uninfected mice, the population of *E. coli* in the ileum

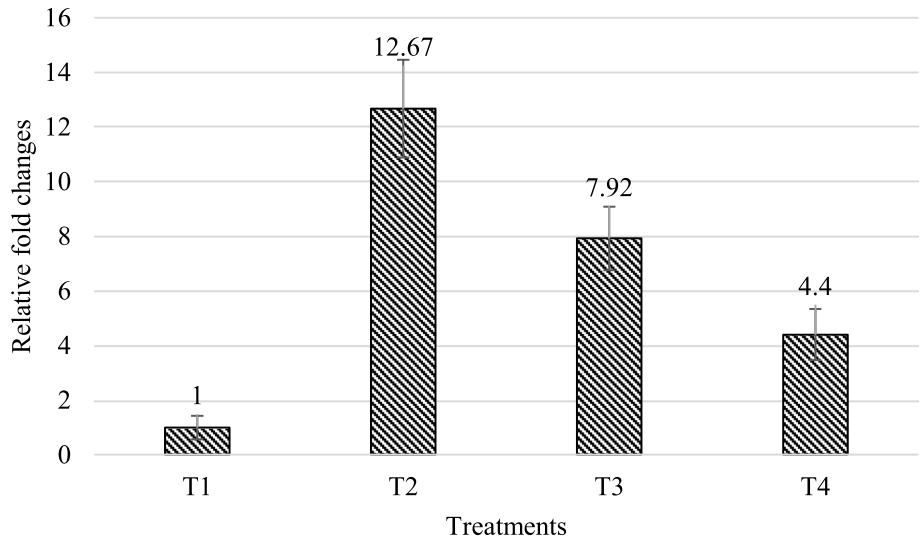

Fig. 3 The relative fold changes in the population of *E. coli* (O157: H7) in the ileum. T1: normal diet. T2: normal diet +infection by *E. coli* (O157: H7) on day 21. T3: a normal diet enriched by a nonencapsulated phenolic-rich fraction (10 mg TPC/kg BW/day) + infection by *E. coli* (O157: H7) on day 21. T4: a normal diet enriched by a nanoliposome-encapsulated phenolic-rich fraction (10 mg TPC/kg BW/day) + infection by *E. coli* (O157: H7) on day 21

of the infected group increased significantly ($p < 0.05$) by 12.6 folds. The dietary supplementation of nonencapsulated PRF and nanoliposome-encapsulated PRF considerably modulated ($p < 0.05$) the population of *E. coli* in the ileum by 7.9 and 4.4 folds, respectively. Seemingly, the nanoliposome-encapsulated PRF was stronger than the nonencapsulated PRF in inhibiting the enteropathogenic *E. coli* population in the ileum. The higher antibacterial activity of nanoliposome-encapsulated PRF as compared to the non-encapsulated PRF could be associated with the higher intestinal solubility and absorption of nanoliposome-encapsulated PRF. Apart from that, as a promising phytobiotic, the nanoliposome-encapsulated PRF could play a role against *E. coli* infection in mice. The inhibition of *E. coli* in the ileum by nanoliposome-encapsulated PRF might be due to the antibacterial activity of the bioactive phenolic compounds in the PRF (Bouarab-Chibane et al. 2019).

Conclusion

The dietary inclusion of the nonencapsulated PRF and the nanoliposome-encapsulated PRF at the concentration of 10 mg TPC/kg BW/day improved the health parameters in mice, which were challenged by enteropathogenic *E. coli*. However, the nanoliposome-encapsulated PRF appeared to be more effective as compared to the nonencapsulated PRF in improving the health parameters. The higher biological activity of nanoliposome-encapsulated PRF could be attributed to the higher intestinal solubility, bioavailability, and absorption of nanoliposome-encapsulated PRF. Consequently, the nanoliposome-encapsulated PRF, as a promising phytobiotic, was found to play a critical role against *E. coli* infection in mice.

Materials and methods

Plant material and reagents

The plant material was obtained from Institute of Medicinal Plant, ACER, Karaj, Iran. Plant identification was carried out by Dr. Majid Ghornabi Nohooji, and the voucher spiceman was deposited in institute of medicinal plant herbarium by 7196-IMPH code number. The soybean lecithin (purity of 99%) was purchased from Sigma Aldrich (Germany). The *E. coli* (O157: H7) was obtained from the microbial culture collection of Islamic Azad University of Mashhad, Iran. For the gene expression analysis, the RNeasy Mini kit (Qiagen, Hilden, Germany), cDNA synthesis Quantitect Reverse Transcription kit (Qiagen, Hilden, Germany), and SYBR Green PCR Master Mix (Qiagen, Hilden, Germany) were used. The DNA extraction kit used in this study was QIAamp DNA Stool Mini Kit from Qiagen GmbH, Hilden, Germany. The other reagents not mentioned here were from Merck (Germany).

Fractionation and total phenolic determination

In the first step, the fresh leaves were cleaned by sterile distilled water, dried in shadow for 2 weeks at room temperature. The dried leaves are finely ground (powder form) using a grinder mill. Then, the 100 g of the dried powder was extracted with 900 mL aqueous methanol (80% (v/v)) and 100 mL of 6 M HCl using the reflux method for 2 h (Karimi et al. 2019). Finally, the extract was filtered and the filtrate was evaporated at the temperature of 60°C by a rotary evaporator (Buchi, Flawil, Switzerland). In the second step, the extract was fractionated using a separating funnel and different solvents including hexane, chloroform, ethyl acetate, n-butanol, and water-based on the Oskoueian et al. (Oskoueian et al. 2020). Upon fractionation, the supernatant was filtered and concentrated using a vacuumed rotary evaporator. The total phenolic compounds (TPC) evaluation of each fraction was carried out by adding 0.1 ml of the extract, 2.5 ml of Folin-Ciocalteu reagent (1:10 v/v), and 2 ml of 7.5% sodium carbonate into a test tube covered with aluminum foil. The test tubes were vortexed and the absorbance was measured at 765 nm (Oskoueian et al. 2020). The results were expressed as milligrams of gallic acid equivalents (GAE) per gram dry weight. The fraction containing the highest phenolic content is named a phenolic rich fraction (PRF).

Nanoliposomes preparation

The 4 g of lecithin was agitated for 2 h by 196 g of hot water (80 °C) using a stirrer at 300 rpm. Then, the PRF after dissolving in ethanol was added to the mixture and stirred for 2 h to reach the final concentration of 2000 ppm. Finally, the solution was bath-sonicated at 80% power (Sonorex RK100, Germany) for 4 to 6 min, and the obtained nanoliposomes-loaded PRF from *A. rosea* was prepared and used for further characterization.

Characterization of nanoliposomes

In the beginning, the nanoliposomes-loaded PRF was diluted by water (1:20) to decrease the aggregation and inhibit noise scattering. The dynamic light scattering (DLS) method was performed to determine the average size of particles and their stability (zeta potential). The measurements were analyzed three times by a Malvern Zetasizer Nano ZS (Malvern, UK). Moreover, field emission scanning electron microscopy (FESEM) was applied to verify the shape and nanoliposomes size dimensions. The total phenolic content of nanoliposomes was determined as described earlier in the fractionation section (Oskoueian et al. 2020).

Phenolic profiling of nanoliposomes

The reversed-phase high-performance liquid chromatography (RP-HPLC) analysis was carried out to

investigate the types of phenolic compounds present in the nanoliposomes. Briefly, in the solvents comprising of deionized water (solvent A) and acetonitrile (solvent B), the pH of solvent A was adjusted to 2.5 using concentrated trifluoroacetic acid. The column was equilibrated by 85% solvent A and 15% solvent B for 15 min before injection. Then, the ratio of solvent B was increased to 85% after 50 min. After 5 min (at the 55th minute of running the experiment), the ratio of solvent B was reduced to 15%. This ratio was maintained for 60 min for the next analysis with a flow rate of 1 ml/min. An analytical column (Intersil ODS-3 5um 4.6 × 150 mm Gl Science Inc. USA) was used for the detection of phenolic at 280 nm. The phenolic standards used in this study were gallic acid, syringic acid, vanillic acid, salicylic acid, caffeic acid, pyrogallol, catechin, cinnamic acid, ellagic acid, naringin, chrysin, and ferulic acid.

Animal trial

The 40 white male Balb/c mice (20–25 g) were obtained from the Razi Vaccine and Serum Research Institute of Mashhad. The mice were kept in separate cages at 23 °C ± 1 °C with 58% ± 10% humidity for 12-h light/dark periods for 7 days for mice to adapt with the lab condition. The mice were divided into four groups of ten with free access to the standard pelleted diet (procured from Javaneh Khorasan, Mashhad, Iran) and tap water. The treatments were as follows:

T1: Normal diet
T2: Normal diet + infected by *E. coli* (O157: H7) on day 21
T3: Normal diet enriched by nonencapsulated PRF (10 mg TPC/kg BW/day) + infected by *E. coli* (O157: H7) on day 21
T4: Normal diet enriched by nanoliposome-encapsulated PRF (10 mg TPC/kg BW/day) + infected by *E. coli* (O157: H7) on day 21

All mice received the experimental treatments for 4 weeks; the oral infection was performed using a gavage needle (10^8 CFU of *C. jejuni*) once on day 21. Animals were monitored daily in terms of their general health and the amount of food eaten. At the end of the experiment (day 28), the mice were euthanized with pentobarbital-HCL (50 mg/kg, i.p.). Immediately, the mice's blood, liver, and ileum samples were collected and used for liver enzyme analysis, lipid peroxidation assay, gene expression analysis, and morphometric evaluation of ileum, respectively. The mice were weighed two times, at the onset and the end of the experiment. All animal experiments were conducted according to the ethical principles approved by the Islamic Azad University of Mashhad (code: IR.IAU.MSHD.REC.1399.016).

Liver enzymes and lipid peroxidation assay

The main liver enzymes in the serum including alanine aminotransferase (ALT), aspartate transaminase (AST), and alkaline phosphatase (ALP) were determined using a blood auto-analyzer (Hitachi 902, Japan). The lipid peroxidation in the liver tissue was determined as described earlier by Shafaei et al. (Shafaei et al. 2020). Briefly, the liver tissue was homogenized and 200 µl of lysate were mixed by distilled water (300 µl), BHT (35 µl), sodium dodecyl sulfate (165 µl), and thiobarbituric acid (2 ml) respectively. Then, after heating (90 °C for 60 min), the cooled solution was mixed with 2 mL of n-butanol and centrifuged at 2000 × *g* for 5 min. Finally, the absorbance of the n-butanol part was read at 532 nm, and the results were expressed as percentage malondialdehyde (MDA) changes relative to the control.

Histopathology and morphometric analyses

At the end of the in vivo experiment, the mice were sacrificed and the liver, kidney, and ileum were separated and washed using the physiological serum. Then, they were fixed in buffered formalin (10% formalin in 0.1 M sodium phosphate buffer, pH 7). Finally, they were paraffinized, sliced, and stained according to the hematoxylin/eosin protocol (Shafaei et al. 2020). The histopathology slides were observed under a light microscope using a magnification of × 20. The morpho-structural characteristics of ileum including villus height, villus width, crypt depth, and goblet cell count were determined (Navarrete et al. 2015).

Gene expression analysis

To investigate the response of ileum tissue to different treatments, the expression of major inflammation biomarker genes such as cyclooxygenase 2 (COX2), inducible nitric oxide synthase (iNOS), and antioxidant-related genes including superoxide dismutase (SOD) and glutathione peroxidase (GPx) was determined. The mice's ileum tissues which were freshly frozen in the liquid nitrogen were crushed and prepared for RNA extraction by an RNeasy Mini kit (Qiagen, Hilden, Germany) following the recommended protocols. Then, cDNA was synthesized using a Quantitect Reverse Transcription kit (Qiagen, Hilden, Germany). Next, the sets of primer sequences for the key genes and housekeeping (beta-actin) gene were applied in the experiment as shown in Table 1. The SYBR Green PCR Master Mix (Qiagen, Hilden, Germany) was used in a comparative

Table 7 The primer sets characteristics used in this study

Gene	Forward (5′→3′)	Reverse (5′→3′)	References
COX2	caagcagtggcaaaggcctcca	ggcacttgcattgatggtggct	Jain et al. 2008
iNOS	caccttggagttcacccagt	accactcgtacttgggatgc	Kou et al. 2011
SOD	gagacctgggcaatgtgact	gtttactgcgcaatcccaat	Kathirvel et al. 2010
GPx	caagtttttgatgccctggt	tcggacgtacttgagggaat	Kathirvel et al. 2010
β-actin	cctgaaccctaaggccaacc	cagctgtggtggtgaagctg	Shafaei et al. 2020

Table 8 The list of the primers used for ileum microbial population analysis

Bacteria	Forward (5′→3′)	Reverse (5′→3′)	References
E. coli (O157:H7)	ttaccagcgataccaagagc	caacatgaccgatgacaagg	Si et al. 2007
Total bacteria	cggcaacgagcgcaaccc	ccattgtagcacg tgtgtagcc	Denman and McSweeney 2006

Real-time PCR (Roche Diagnostics). The targeted genes were amplified as follows: 95 °C for 5 min (1X) for initial denaturation, followed by 35 cycles of 95 °C for the 30s, primer annealing at 60 and 58 for 30 s for the inflammatory genes and antioxidant genes, respectively, and extension of 72 °C for 30s. The expressions of genes were normalized to beta-actin as a reference gene and then normalized to the expression of respective genes in the control group (Kathirvel et al. 2010). The characteristics of the primer used in this study are presented in Table 7.

E. coli population analysis

The real-time PCR (LightCycler 96 instrument, Roche, Basel, Switzerland) was used to determine the fold changes of the *E. coli* (O157: H7) population in the ileal digesta, since the major sites of microbial fermentation and propagation and colonization of enteropathogens in the monogastric is the ileum, which is why in this study, the population of *E. coli* was analyzed only in the ileum section. The real-time PCR condition was 95 °C for 5 min (1X) for initial denaturation, followed by 35 cycles of 95 °C for the 30s, primer annealing at 60, and 55 for 25 s for the *E. coli* and total bacteria, respectively, and extension of 72 °C for 20s. The primer characteristics are shown in Table 8. The DNA from ileum digesta was extracted using QIAamp DNA Stool, extraction kit (QIAGEN, Germany). The SYBR GREEN Master Mix (BIOFACT, Korea) was used in this study. The previously published primers were used for quantitative real-time PCR assay. The real-time PCR data were analyzed using ΔΔCt method to determine the fold changes in the *E. coli* bacteria population, and the data were expressed as fold changes of *E. coli* relative to the total bacteria (Feng et al. 2010; Si et al. 2007).

Statistical analysis

The data obtained were subjected to the general linear models (GLM) procedure of SAS [(9.1) (2002-2003) (SAS Institute Inc., Cary, NC, USA)] in a completely randomized design (CRD), and the means were compared with Duncan's multiple range test. The difference was considered significant when the p-value was < 0.05.

Acknowledgements

The authors are grateful to the Islamic Azad University of Mashhad for the laboratory facilities.

Authors' contributions

NH: study design, experimental work, and writing original draft; EK and EO: analysis, methodology, project administration, supervision, review, and editing of the original draft; All authors read and approved the final manuscript.

Funding

There has been no financial support for this work.

Availability of data and materials

The datasets applied during the current study are available on reasonable request.

Declarations

Ethics approval and consent to participate

All protocols to use the in vivo study were reviewed and reported in accordance with ARRIVE guidelines. All animal experiments were conducted according to the ethical principles approved by the Islamic Azad University of Mashhad, IRAN with the code of ethics IR.IAU.MSHD.REC.1399.016.

Consent for publication

Not applicable.

Competing interests

The authors declare that they have no competing interests.

Author details

[1]Department of Biology, Mashhad Branch, Islamic Azad University, Mashhad, Iran. [2]Department of Research and Development, Arka Industrial Cluster, Mashhad, Iran.

Received: 9 September 2021 Accepted: 1 February 2022
Published online: 21 February 2022

References

Abdel-salam NA, Ghazy NM, Sallam SM et al (2018) Flavonoids of Alcea rosea L. and their immune stimulant, antioxidant and cytotoxic activities on hepatocellular carcinoma HepG-2 cell line. Natural Product Research 32:702–706

Abdelwahab SI, Mohan S, Mohamed Elhassan M et al. (2010) Antiapoptotic and antioxidant properties of Orthosiphon stamineus benth (Cat's Whiskers): intervention in the Bcl-2-mediated apoptotic pathway. Evidence-Based Complementary and Alternative Medicine 2011

Acosta-Estrada BA, Gutiérrez-Uribe JA, Serna-Saldívar SO (2014) Bound phenolics in foods, a review. Food Chemistry 152:46–55

Aditya N, Espinosa YG, Norton IT (2017) Encapsulation systems for the delivery of hydrophilic nutraceuticals: food application. Biotechnol Advances 35:450–457

Ahmadi M, Rad AK, Rajaei Z et al (2012) Alcea rosea root extract as a preventive and curative agent in ethylene glycol-induced urolithiasis in rats. Indian J Pharmacol 44:304

Anand S, Deighton M, Livanos G et al (2019) Antimicrobial activity of Agastache honey and characterization of its bioactive compounds in comparison with important commercial honeys. Front Microbiol 10:263

Azab A (2017) Alcea: Traditional medicine, current research and future opportunities. Eur Chem Bull 5:505–514

Bouarab-Chibane L, Forquet V, Lantéri P et al (2019) Antibacterial properties of polyphenols: characterization and QSAR (Quantitative structure–activity relationship) models. Front Microbiol 10:829

Cianciosi D, Forbes-Hernández TY, Afrin S et al (2018) Phenolic compounds in honey and their associated health benefits: a review. Molecules 23:2322

Denman SE, McSweeney CS (2006) Development of a real-time PCR assay for monitoring anaerobic fungal and cellulolytic bacterial populations within the rumen. FEMS MicrobiolEcol 58:572–582

Emami S, Azadmard-Damirchi S, Peighambardoust SH et al (2016) Liposomes as carrier vehicles for functional compounds in food sector. J Experimental Nanosci 11:737–759

Erlwanger K, Cooper R (2008) The effects of orally administered crude alcohol and aqueous extracts of African potato (Hypoxis hemerocallidea) corm on the morphometry of viscera of suckling rats. Food Chem Toxicol 46:136–139

Feng Y, Gong J, Yu H et al (2010) Identification of changes in the composition of ileal bacterial microbiota of broiler chickens infected with Clostridium perfringens. Veterinary Microbiol 140:116–121

Figueroa-Robles A, Antunes-Ricardo M, Guajardo-Flores D (2021) Encapsulation of phenolic compounds with liposomal improvement in the cosmetic industry. Int J Pharmaceutics 593:120125

Fischbach MA, Walsh CT (2009) Antibiotics for emerging pathogens. Science 325:1089–1093

Friedman ND, Temkin E, Carmeli Y (2016) The negative impact of antibiotic resistance. Clin Microbiol Infection 22:416–422

Frieri M, Kumar K, Boutin A (2017) Antibiotic resistance. J Infection Public Health 10:369–378

Górniak I, Bartoszewski R, Króliczewski J (2019) Comprehensive review of antimicrobial activities of plant flavonoids. Phytochem Rev 18:241–272

Gutiérrez-del-Río I, Fernández J, Lombó F (2018) Plant nutraceuticals as antimicrobial agents in food preservation: terpenoids, polyphenols and thiols. Int J Antimicrobial Agents 52:309–315

Hadi MY, Hameed IH, Ibraheam IA (2017) Mentha pulegium: medicinal uses, anti-hepatic, antibacterial, antioxidant effect and analysis of bioactive natural compounds: a review. Res J Pharm Technol 10:3580–3584

Hasan M, Belhaj N, Benachour H et al (2014a) Liposome encapsulation of curcumin: physico-chemical characterizations and effects on MCF7 cancer cell proliferation. Int J Pharmaceutics 461:519–528

Hasan M, Belhaj N, Benachour H et al. (2014b) Liposome encapsulation of curcumin: physico-chemical characterizations and effects on MCF7 cancer cell proliferation. 461:519-528

Hashemi Z, Shirzadi-Ahoodashti M, Ebrahimzadeh MA (2021) Antileishmanial and antibacterial activities of biologically synthesized silver nanoparticles using Alcea rosea extract (AR-AgNPs). J Water Environmental Nanotechnol 6:265–276

Hassan A, Ojo B, Abdulrahman A (2021) Escherichia coli as a global pathogen. Achievers J Scientific Research 3:239–260

Hwang IY, Koh E, Wong A et al (2017) Engineered probiotic Escherichia coli can eliminate and prevent Pseudomonas aeruginosa gut infection in animal models. Nature Communications 8:1–11

Jain NK, Ishikawa T-O, Spigelman I et al (2008) COX-2 expression and function in the hyperalgesic response to paw inflammation in mice. Prostaglandins, Leukotrienes Essential Fatty Acids 79:183–190

Ju H-Y, Chen SC, Wu K-J et al (2012) Antioxidant phenolic profile from ethyl acetate fraction of Fructus Ligustri Lucidi with protection against hydrogen peroxide-induced oxidative damage in SH-SY5Y cells. Food Chem Toxicol 50:492–502. https://doi.org/10.1016/j.fct.2011.11.036

Karimi E, Mehrabanjoubani P, Es-Haghi A et al (2019) Phenolic compounds of endemic buxus plants in caspian hyrcanian forest (Buxus Hyrcana Pojark) and their biological activities. Pharmaceutical Chem J 53:741–747

Kathirvel E, Chen P, Morgan K et al (2010) Oxidative stress and regulation of anti-oxidant enzymes in cytochrome P4502E1 transgenic mouse model of non-alcoholic fatty liver. J Gastroenterol Hepatology 25:1136–1143

Kaur R, Arora S, Singh B (2008) Antioxidant activity of the phenol rich fractions of leaves of Chukrasia tabularis A. Juss Bioresource Technol 99:7692–7698. https://doi.org/10.1016/j.biortech.2008.01.070

Khan I, Zaneb H, Masood S et al. (2017) Effect of Moringa oleifera leaf powder supplementation on growth performance and intestinal morphology in broiler chickens. J Animal Physiol Animal Nutrition 101:114-121

Khoshnamvand M, Ashtiani S, Huo C et al. (2019) Use of Alcea rosea leaf extract for biomimetic synthesis of gold nanoparticles with innate free radical scavenging and catalytic activities. J Mol Structure 1179:749-755

Kou X, Qi S, Dai W et al. (2011) Arctigenin inhibits lipopolysaccharide-induced iNOS expression in RAW264. 7 cells through suppressing JAK-STAT signal pathway. Int Immunopharmacol. 11:1095-1102

Kumar A, Dixit CK (2017) Methods for characterization of nanoparticles. In: Advances in nanomedicine for the delivery of therapeutic nucleic acids. Elsevier, pp 43-58

Lim T (2014) Alcea rosea. In: Edible medicinal and non medicinal plants. Springer, pp 292-299

Mariem S, Hanen F, Inès J et al. (2014) Phenolic profile, biological activities and fraction analysis of the medicinal halophyte Retama raetam. South Afr J Botany 94:114-121 doi:https://doi.org/10.1016/j.sajb.2014.06.010

Mostafa AA, Al-Askar AA, Almaary KS et al. (2018) Antimicrobial activity of some plant extracts against bacterial strains causing food poisoning diseases. Saudi J Biol Sci 25:361-366

Navarrete J, Vásquez B, Del Sol M (2015) Morphoquantitative analysis of the Ileum of C57BL/6 mice (Mus musculus) fed with a high-fat diet. Int J Clin Experimental Pathol 8:14649

Nicolau AI, Gostin AI (2016) Safety of edible flowers. In: Regulating safety of traditional and ethnic foods. Elsevier, pp 395-419

Nofrarias M, Manzanilla E, Pujols J et al (2006) Effects of spray-dried porcine plasma and plant extracts on intestinal morphology and on leukocyte cell subsets of weaned pigs. J Animal Sci 84:2735–2742

Olatunji OJ, Chen H, Zhou Y (2017) Effect of the polyphenol rich ethyl acetate fraction from the leaves of Lycium chinenseMill. on Oxidative stress, dyslipidemia, and diabetes mellitus in streptozotocin-nicotinamide induced diabetic rats. Chem Biodiversity 14:e1700277

Oskoueian E, Karimi E, Noura R et al (2020) Nanoliposomes encapsulation of enriched phenolic fraction from pistachio hulls and its antioxidant, anti-inflammatory, and anti-melanogenic activities. J MicroenCapsulation 37:1–13

Ozkan G, Franco P, De Marco I et al (2019) A review of microencapsulation methods for food antioxidants: principles, advantages, drawbacks and applications. Food Chemistry 272:494–506

Pogány Simonová M, Chrastinová Ľ, Kandričáková A et al (2020) Can enterocin M in combination with sage extract have beneficial effect on microbiota, blood biochemistry, phagocytic activity and jejunal morphometry in broiler rabbits? Animals 10:115

Rafiee Z, Barzegar M, Sahari MA et al (2017) Nanoliposomal carriers for improvement the bioavailability of high–valued phenolic compounds of pistachio green hull extract. Food Chem 220:115–122

Rubió L, Motilva M-J, Romero M-P (2013) Recent advances in biologically active compounds in herbs and spices: a review of the most effective

antioxidant and anti-inflammatory active principles. Critical Reviews Food Sci Nutrition 53:943–953
Salimi A (2018) Liposomes as a novel drug delivery system: fundamental and pharmaceutical application. Asian Journal of Pharmaceutics (AJP): Free full text articles from Asian J Pharm 12
Sarı A, Şahin H, Özsoy N et al (2019) Phenolic compounds and in vitro antioxidant, anti-inflammatory, antimicrobial activities of Scorzonera hieraciifolia Hayek roots South African. J Botany 125:116–119
Shafaei N, Barkhordar SMA, Rahmani F et al. (2020) Protective effects of Anethum graveolens seed's oil nanoemulsion against cadmium-induced oxidative stress in mice. Biological Trace Element Research:1-9
Si C, Kun-Lun H, Wen-Tao X et al (2007) Real-time quantitative PCR detection of Escherichia coli O157: H7. Chin J Agricultural Biotechnol 4:15–19
Tuba M, Fafal T, KIVÇAK B et al. (2010) Antimicrobial and cytotoxic activities of the extracts obtained from the flowers of Alcea rosea L. Hacettepe University J Faculty of Pharm:17-24
Vadhana P, Singh B, Bharadwaj M et al (2015) Emergence of herbal antimicrobial drug resistance in clinical bacterial isolates. Pharm Anal Acta 6:434
Zhang Y, Jin L, Chen Q et al (2015) Hypoglycemic activity evaluation and chemical study on hollyhock flowers. Fitoterapia 102:7–14

Publisher's Note